

Computational studies on gas phase polyborate anions

Beckett, M.A.; Davies, R.A.; Thomas, C.D.

Computational and Theoretical Chemistry

DOI:

[10.1016/j.comptc.2014.06.010](https://doi.org/10.1016/j.comptc.2014.06.010)

Published: 22/06/2014

Peer reviewed version

[Cyswllt i'r cyhoeddiad / Link to publication](#)

Dyfyniad o'r fersiwn a gyhoeddwyd / Citation for published version (APA):

Beckett, M. A., Davies, R. A., & Thomas, C. D. (2014). Computational studies on gas phase polyborate anions. *Computational and Theoretical Chemistry*, 1044, 74-79. <https://doi.org/10.1016/j.comptc.2014.06.010>

Hawliau Cyffredinol / General rights

Copyright and moral rights for the publications made accessible in the public portal are retained by the authors and/or other copyright owners and it is a condition of accessing publications that users recognise and abide by the legal requirements associated with these rights.

- Users may download and print one copy of any publication from the public portal for the purpose of private study or research.
- You may not further distribute the material or use it for any profit-making activity or commercial gain
- You may freely distribute the URL identifying the publication in the public portal ?

Take down policy

If you believe that this document breaches copyright please contact us providing details, and we will remove access to the work immediately and investigate your claim.

Computational studies on gas phase polyborate anions

Michael A. Beckett,* R. Andrew Davies* and Christopher D. Thomas

School of Chemistry, Bangor University, Bangor, Gwynedd, LL57 2UW, UK

*Corresponding authors: m.a.beckett@bangor.ac.uk; r.a.davies@bangor.ac.uk

Abstract

The borate anions $[\text{B}(\text{OH})_4]^-$, $[\text{B}_2\text{O}(\text{OH})_5]^-$, $[\text{B}_3\text{O}_3(\text{OH})_4]^-$, $[\text{B}_3\text{O}_3(\text{OH})_5]^{2-}$, $[\text{B}_3\text{O}_3(\text{OH})_6]^{3-}$, $[\text{B}_4\text{O}_5(\text{OH})_4]^{2-}$, $[\text{B}_5\text{O}_6(\text{OH})_4]^-$, and $[\text{B}_7\text{O}_9(\text{OH})_5]^{2-}$ (2 isomers) and the neutral orthoboric and metaboric acids, $\text{B}(\text{OH})_3$ and $\text{B}_3\text{O}_3(\text{OH})_3$, have been structurally optimised in the gas phase at the B3LYP/6-311++G(*d,p*) level. Energetic data, combined with analogous data for ‘building blocks’ H_2O and $[\text{OH}]^-$, has enabled their relative gas phase stabilities (all exothermic) to be determined using an isodesmic approach as: $[\text{B}_5\text{O}_6(\text{OH})_4]^- > [\text{B}_3\text{O}_3(\text{OH})_4]^- > [\text{B}(\text{OH})_4]^- > [\text{B}_7\text{O}_9(\text{OH})_5]^{2-} > [\text{B}_4\text{O}_5(\text{OH})_4]^{2-} > [\text{B}_3\text{O}_3(\text{OH})_5]^{2-}$. The two isomers of $[\text{B}_7\text{O}_9(\text{OH})_5]^{2-}$ have similar total energies although the ‘ribbon’ isomer is calculated to be more stable by only 10.0 kJ mol⁻¹. QTAIM analyses have been undertaken on all computed structures, and QTAIM charges for H, O and B atoms have been calculated. It is concluded that H-bond interactions dominate the solid-state energetics of non-metal cation polyborate salts.

Keywords: polyborate; DFT; QTAIM charges; B3LYP; QTAIM analysis; H-bonding.

1. Introduction

Polyborate anions may be classified as ‘condensed’ or ‘isolated’ with condensed anions being polymeric in structure whereas isolated anions are separated anionic entities [1]. Isolated anions have been observed in the gas phase in MS studies [2] and have also been characterized by XRD studies [3,4] as crystalline salts with either metal or non-metal counterions. Isolated polyborate anions in aqueous solution are less well characterized, in that dissolution of $B(OH)_3$ in basic aqueous solution results in a set of complex equilibria reactions involving a number of polyborate species which also rapidly undergo solvent exchange reactions [5]. These equilibrated dynamic mixtures have been studied by a variety of experimental techniques including ^{11}B NMR [6], potentiometric titrations/temperature jump rate studies [7], X-ray scattering [8], and vibrational [9,10] spectroscopy. The equilibrium concentrations of the various polyborates are dependent upon the total boron concentration, pH, and temperature [11], and as such present a anionic Dynamic Combinatorial Library (DCL) [12] from which, in the presence of suitable cations, energetically favourable isolated polyborate salts will crystallize. We are interested in preparing non-metal cation polyborate salts, as possible thermal precursors to porous materials [13], and have instigated this preliminary computational study to determine the relative stabilities of these isolated polyborate anions. Zhou *et al.* have recently performed a DFT study on a series of isolated polyborate anions in both gas phase and aqueous phase at the B3LYP/aug-cc-pVDZ level [10]. Since isolated polyborate anions are strongly solvated in aqueous solution, and are not solvated in the solid-state, we have chosen a gas phase study (where the isolated anions are truly isolated) to model their intrinsic relative stabilities. In addition, these gas phase calculations will give insight into the bonding and intermolecular interactions within these isolated anions. The anions were modelled with a gas phase DFT study using Gaussian 09 [14] computational software using the B3LYP functional and a 6-

311++G(*d,p*) basis set. During the modelling, particular care was taken when positioning the hydrogen atoms. Each rotamer of each borate was computed, the intermolecular interactions explored, and hence the lowest energy state of the molecule was found. Such interactions include potential hydrogen bonding, hydrogen-hydrogen bonding [15-17] and oxygen to oxygen partial bonding which has recently been observed [18]. AIM2000 [19,20] is a software package based on Quantum Theory of Atoms in Molecules (QTAIM) developed by Bader [21-23] which can be utilized to characterise these internal interactions. The results obtained are compared with the calculations of Zhou *et al.* [10]. Two isomers of $[\text{B}_7\text{O}_9(\text{OH})_5]^{2-}$, partnered by metallic and/or non-metal cations, have recently been synthesised and characterised by X-ray diffraction studies [24-28]. These anions are illustrated in Figure 1. These isomers are referred to in this manuscript as the as a ‘ribbon’ isomer [24-26] and an ‘O⁺’ isomer [27,28]. We were interested in investigating their relative energies by a detailed DFT study and the results are reported herein. The DFT calculations indicate that the two isomers are of approximately equal energy. The ‘O⁺’ isomer was of particular interest as the reported structure [27,28] has three 4-coordinate and formally negatively charged B centres and one 3-coordinate O atom with a formal positive charge, in order to maintain the 2- dianion charge. QTAIM charge distributions for this isomer has been obtained, and these calculations demonstrate that all bridging O atoms bound to tetrahedral B atoms (including the formally positive O atom), possess similar and substantial negative charges, with the positive charges located on the more electropositive B and H centres.

2. Experimental methods

2.1 General. The Gaussian 09 software package was employed to perform electronic structure and geometry optimisation calculations on the polyborate anions [14]. In order to

increase computational efficiency, initial geometry optimisations were performed using the AM1 semi-empirical Hamiltonian. In order to obtain accurate descriptions of intramolecular hydrogen bonding, subsequent Density Functional Theory (DFT) calculations employing the Becke-Lee-Yang-Parr (B3LYP) functional combined with a Pople-type 6-311++G(*d,p*) basis set were performed on the aforementioned optimised structures [29-31]. All molecules were modelled in the gas-phase under vacuum conditions. Energies were converted (1 a.u. = 1 Ha = 2625.5 kJ mol⁻¹) as required. Analysis of the output files were conducted using GaussView 5.0 [32] and AIM2000 [33]. QTAIM charges were obtained using AIM2000 by natural coordinate integration of the atomic bases. For completeness, the energies of H₂O and [OH]⁻ were calculated by the same methods as -76.458531 and -75.827448 a.u., respectively.

2.2 Computational strategy for determining global minima. The molecules/anions to model were divided into two classes: fundamental building blocks and larger composite polyborates. The fundamental building blocks were chosen so that the results would provide valuable information on what should be expected when modelling the larger systems. B(OH)₃ (**1**), [B(OH)₄]⁻ (**2**), B₂O(OH)₄ (**3**), B₃O₃(OH)₃ (**5**) and [B₅O₆(OH)₄]⁻ (**10**) were chosen as ‘fundamental building blocks’ as they illustrated particular structural features with more general applicability. Thus, **1** and **2** were the smallest of the ‘polyborates’ with trigonal and tetrahedral (charged) B centers, **3** was the simplest molecule to have a ring created by hydrogen bonding, **5** had O atoms bridging B centers in a boroxole ring, and **10** was the simplest molecule with a tetrahedral (charged) boron not bonded to a hydroxyl group. Torsional 1-D scans were performed for each successive hydroxyl groups within the polyborates, confirming that the minima (see Supplementary Data) were co-planar with B-O bonds around trigonal B centers. Hydroxyl groups in tetrahedral B centres have previously been investigated [34], and all rotamers were again examined to determine the global minimum (see Supplementary Data). The composite polyborates consisted of [B₂O(OH)₅]⁻

(**4**), $[\text{B}_3\text{O}_3(\text{OH})_4]^-$ (**6**), $[\text{B}_3\text{O}_3(\text{OH})_5]^{2-}$ (**7**), $[\text{B}_3\text{O}_3(\text{OH})_6]^{3-}$ (**8**), $[\text{B}_4\text{O}_5(\text{OH})_4]^{2-}$ (**9**), and $[\text{B}_7\text{O}_9(\text{OH})_5]^{2-}$ (2 isomers, **11** and **12**). The diborate(1-) **4** was approached by dividing the molecule into two through the bridging oxygen, with each half of the molecule having four possible orientations. Triborate(1-) (**6**) was separated into two parts: one contained the tetrahedral boron, the other contained the trigonal boron. The former had two orientations and the latter contained three. The triborate(2-) (**7**) resembled **3** and rotamers were obtained by a similar procedure. The triborate(3-) (**8**) and tetraborate(2-) (**9**) had only one way of arranging the hydroxyl groups to give minimum rather than transition structures. The ‘ribbon’ isomer of the heptaborate(2-) (**11**) was modelled in the same way as the pentaborate(1-) (**10**) with the central hydroxyl group kept in the plane of the central ring. The ‘O⁺’ isomer of the heptaborate(2-) (**12**) was more complex. All hydroxyl groups on trigonal borons were kept planar with respect to an adjacent oxygen and pointing in a ring, in a similar fashion to metaboric acid (**5**). This remaining hydroxyl group was then rotated using a 1-D torsional scan to find the most likely location of its hydrogen atom. Full information of all rotamers of all compounds is given in as Supplementary Data.

3. Results and Discussion

3.1 Global minima and QTAIM analysis. Zhou and co-workers have investigated polyborates in the gas phase and in aqueous solution by DFT methods [10]. Their results indicated that the calculations were comparable in relative terms although solvated ions were always more stable than unsolvated gas phase ions. In our preliminary calculations we have examined these polyborate anions also in the gas phase using a higher quality basis set, as a means of further modelling these isolated polyborate anions. The global minimum for all the polyborate species is shown in Figure 2 and their energies are given in the caption. In general our calculations are in agreement with those of Zhou and co-workers [10]. As a result of our

detailed rotamer analysis we did observe different global minima for compounds **4**, **5**, **8**, and **10**.

QTAIM analysis can be used to give an indication of the relative strength of an interaction between two nuclei by comparing the electron density at the bond critical point (BCP), ρ_b . Smaller electron density values, bond and ring critical point (RCP) coalescence or the lack of a bond critical point between two nuclear critical points generally indicate weak interactions. The Laplacian of the electron density, $\nabla^2(\rho_b)$, is calculated by summing the eigenvalues (λ_1 , λ_2 and λ_3) of the Hessian matrix [23]. A negative value of the Laplacian indicates a concentration of electron density *i.e.* a covalent interaction. A positive value of the Laplacian indicates a depletion of charge *i.e.* a closed-shell electrostatic interaction *e.g.* a hydrogen bond. The bond ellipticity, ε , measures the extent to which density is preferentially accumulated in a given plane containing the bond path, with zero values for cylindrically symmetric single and triple bonds, and larger values for double bonds. QTAIM molecular graphs depicting bond paths and critical points for the polyborate anions/molecules are shown in Figure 3. In general, hydroxyl groups within polyborate anions were at a minimum energy when co-planar with other B-O bonds at trigonal B centres. This often resulted in 4 membered rings with short OH \cdots O intermolecular contacts. These interactions are present in **1** and QTAIM analysis showed that these interactions are predominantly electrostatic in origin since there was no evidence for a formal H-bonding or hydrogen-hydrogen bonding. Likewise, although non-planar, the 4-membered ring OH \cdots O interactions in **2** are electrostatic in origin.

There are ten unique ways that the co-planar hydroxyl groups can be arranged around the B₂O centre in **3**. The global minimum is stabilized by the presence of a 6-membered ring intramolecular H-bond, which is apparent from QTAIM analysis.

Geometry optimisation of diborate(1-) (**4**) revealed five unique co-planar rotamers.

The lowest energy rotamer has the largest distance between the BCP of the hydrogen bond and the RCP, indicating stable ring formation. Harmonic vibrational frequency analysis of the O-H bonds showed a large red shift of $\sim 400\text{ cm}^{-1}$, which when coupled with an extension of the O-H bond length by $\sim 0.02\text{ \AA}$, clearly indicates the presence of intramolecular hydrogen bond in **4**.

There are two planar conformers of metaboric acid (**5**) with the one possessing C_{3h} symmetry being the global minimum. QTAIM analysis revealed that a RCP is present in the middle of the boron-oxygen ring, and that the 4-membered ring OH \cdots H interactions were again electrostatic in origin with no formal H-bonds.

There are six rotamers for the triborate(1-) anion (**6**) with the global minimum possessing two interactions to a ring oxygens (one of these is weaker with the b' interaction being $\sim 0.235\text{ \AA}$ longer). QTAIM analysis indicated that there were no additional interactions other than the expected RCP of the boroxole ring.

The six rotamers of triborate(2-) (**7**) form a second 6-membered ring comprising of a hydrogen bond. The relative energy of these rotamers only vary by $<11\text{ kJ mol}^{-1}$, and this energy difference is comparable to available thermal energy. The minimum energy rotamer possesses the strongest hydrogen bond with the electron density at its BCP and the distance between the BCP and RCP being the greatest. There is a small OH vibrational red shift of $\sim 100\text{ cm}^{-1}$ and an extension of the O-H bond length. QTAIM analysis of similar rotamers of the triborate(3-) (**8**) did not reveal evidence of hydrogen bonding or changes in bond lengths/vibrational frequencies.

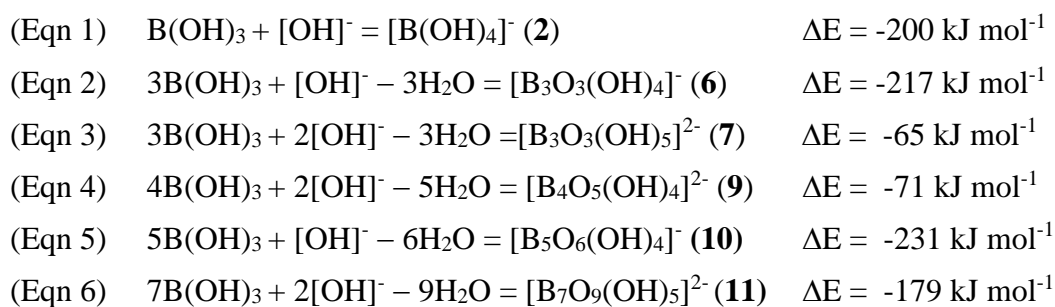
The optimised structure for tetraborate(2-) (**9**) can be likened to two molecules of **5** conjoined and sharing a common backbone with the hydroxyls pointing in a ring to create a mirror plane. Two RCPs are observed and all the 4-membered ring OH \cdots O interactions appear electrostatic in origin.

The pentaborate(1-) (**10**) anion has six unique rotamers with hydroxyl groups coplanar. In the global minimum conformation, the presence of RCPs near to, or at the centres of the boroxole rings, confirm the formation of stable ring systems, but the absence of BCPs indicate that the 4-membered ring O-H \cdots O interactions are electrostatic in origin.

The ten rotamers of the heptaborate(2-) ‘ribbon’ isomer (**11**) have an energy range of 46 kJ mol⁻¹. The minimum has the hydroxyl groups pointing inwards in a similar fashion to the minimum of **10**. Again, the presence of ring critical points near to, or at the centres of the boroxole rings, confirming the formation of stable ring systems was demonstrated by QTAIM analysis, but there was no evidence for any intramolecular hydrogen bonding.

A 1-D torsional scan was performed on the heptaborate(2-) ‘O⁺’ (**12**) by rotating the O-H group relative to the B-O⁺ bond. The minima were located at $\pm 50^\circ$, pointing towards O atoms, and the energy difference between the two rotamers is *ca.* 2 kJ mol⁻¹, which is below the threshold of computational error. Both rotamers possess a very weak, yet stabilising hydrogen bond, with the stronger of the two giving rise to the global minimum. There was no noticeable increase in the O-H bond length, but there was a weak red shift of ~ 15 cm⁻¹. The ‘ribbon’ isomer is more stable than the ‘O⁺’ isomer by 10 kJ mol⁻¹ despite the ‘O⁺’ isomer having an additional hydrogen bond (interaction e’).

3.2 Relative stability of gas phase polyborate anions. The calculated total energies for the polyborate anions show a large increase as the number of atoms increase. However, this does not allow for a direct comparison of their relative gas phase stabilities, *per se*. One way of doing so is to compare the calculated energies of an anion with the sum of its calculated components, as shown in Equations 1-6. In order to do so, the total energies of H₂O (-200,742 kJ mol⁻¹) and [OH]⁻ (-199,085 kJ mol⁻¹) were calculated using an identical B3LYP/6-311++G(*d,p*) methodology. The lower energy heptaborate (2-) ‘ribbon’ isomer (**11**) is used in the calculation in Eqn. 6.



These calculations, which give absolute energies relative to the fundamental building blocks, indicate that formation of the pentaborate(1-) anion (**10**), is energetically the most favoured in the gas phase, and in general, monoanions are favoured over dianions. The overall energy order is as follows: **10** < **6** < **2** < **11** < **9** < **7**, indicating that **10** is more stable than **7**. Such an approach however, fails to appreciate the number of B atoms in the polyborate anion since the pentaborate in absolute terms is only marginally more stable than the triborate (and monoborate) which contain fewer B atoms. An average relative energy *per B atom*, gives a better approximation of relative energies in the gas phase of the polyborates per B unit and the following ordered is obtained: **2** (-200 kJ mol⁻¹) < **6** (-72 kJ mol⁻¹) < **10** (-46 kJ mol⁻¹) < **11** (-25 kJ mol⁻¹) < **7** (-21 kJ mol⁻¹) < **9** (-18 kJ mol⁻¹).

Pure single polyborate salts, containing isolated anions, often crystallise from the DCL of anions present in aqueous solution through self-assembly processes [13]. It should be noted that polyborate ions **2**, **6**, **7** and **9** are only observed under highly basic conditions in aqueous solution [7][35]. In agreement with the relatively high stability of **10**, non-metal cation pentaborate salts are most readily obtained from aqueous solution at moderate pH. However, care must be taken with this gas phase computational approach to the isolated anions as it ignores intermolecular H-bond interactions (anion-anion, cation-anion and cation-cation) which probably dominate the energetics in the solid-state. NMC pentaborate salts often contain supramolecular H-bonded giant lattices, and even in situations when the cation does not partake in any H-bond interactions *e.g.* $[O(CH_2CH_2)_2NMe_2][\mathbf{10}]$ [13], each pentaborate anions will accept four strong acceptor H bonds (3 at α and 1 at β sites [36])

from its pentaborate neighbours in a ‘herringbone’ structure, and thus reducing the overall energy of the salt by say $\sim 100 \text{ kJ mol}^{-1}$ (at 25 kJ mol^{-1} per interaction). There are ten potential H-bond acceptor sites in **10**. $[\text{PhCH}_2\text{NH}_3][\mathbf{10}]$ has a similar ‘herringbone’ pentaborate [37] lattice to $[\text{O}(\text{CH}_2\text{CH}_2)_2\text{NMe}_2][\mathbf{10}]$ but each cation forms 3 additional H-bond interactions to an anion (at α , β and β/γ bifurcated sites) clearly influencing its overall stability. Similarly, extensive H-bonding interactions can be found in the solid-state structure of $[\text{4-MepyH.4-Mepy}][\mathbf{10}]$ and $[\text{Me}_3\text{NCH}_2\text{CH}_2\text{OH}][\mathbf{10}]$ [38]. Such multi-point H-bond interactions cannot be overemphasised and a simple analysis of the eight single-crystal X-ray structures presented in reference [13] reveals that all of the potential H-bond donor sites of the cations are involved in H-bonding in their solid-state structures with the anion on average having six of its ten potential acceptor sites utilized. The QTAIM charges for pentaborate(1-) **10** have been calculated and the formally negative 4-coordinate B centre has marginally the largest positive charge, at $+2.30e$. The α , β and γ O atoms have negative charges of $-1.55e$, $-1.29e$ and $-1.54e$ respectively, and the 3-coordinate B centres are positive at $+2.27e$. The balance of the charges, to make a 1- anion, is made up by H atoms ($+0.56e$). These atomic charges are not too dissimilar to the those calculated (QTAIM) for $\text{B}(\text{OH})_3$ (**1**) which has O atoms negatively charged ($-1.34e$) and the B and H atoms positively charged at $+2.28e$ and $+0.58e$, respectively. The α -sites in the pentaborate anions, which carry the largest negative charge, are the usual preferred H bond interaction sites, but such interactions are enhanced by reciprocal pair $\text{R}_2^2(8)$ Etter interactions [39], similar to those found in carboxylic acid dimers. H-bond interactions to γ -sites occur less frequently, although the calculated charges on these O atoms are only slightly less negative.

The heptaborate(2-) anion (both isomers) also have ample opportunity to accept H-bond interactions with fourteen potential acceptor sites. Again an analysis of reported non-metal cation heptaborate salts show that 12 out of the 14 (12/14) potential heptaborate

acceptor sites are used in $[\text{H}_2\text{en}]_2[\mathbf{11}].[\text{B}_4\text{O}_5(\text{OH})_4].3\text{H}_2\text{O}$ [26], and 11/14, 10/14 and 10/14 acceptor sites are utilized for $[\text{cyclo-C}_6\text{H}_{11}\text{NH}_3]_2[\mathbf{12}].3\text{H}_2\text{O}.\text{B}(\text{OH})_3$ [28] and $[\text{cyclo-C}_7\text{H}_{13}\text{NH}_3]_2[\mathbf{12}].2\text{H}_2\text{O}.2\text{B}(\text{OH})_3$ [28] and $[\text{H}_3\text{N}(\text{CH}_2)_7\text{NH}_3][\mathbf{12}].3\text{H}_2\text{O}$ [27], respectively. The QTAIM charges for **12** have been calculated and the charge distribution is very similar to that obtained for **10**. The trigonal B centres carry positive charge of +2.26e, H atom +0.54, and hydroxyl O atoms -1.28e. The structurally unique 3-coordinate O atom in **12** carries a large negative charge (-1.53e) and is surrounded by three 4-coordinate B centres with large positive charges (+2.30e). Interestingly, this 3-coordinate O (bridging 3 B_{tet} centres), with its formal +ve charge, has a similar negative charge to other bridging O atoms (bridging B_{tet} and B_{trig} centres, -1.54e) in the anion.

$[\text{H}_2\text{en}]_2[\mathbf{11}].[\mathbf{9}].3\text{H}_2\text{O}$ [26] is also a rare example of a non-metal cation tetraborate salt. The tetraborate(2-) (**9**) has 9/9 H-bond acceptor sites utilized in this solid-state structure. The QTAIM charge distribution for the structurally unique O atom, which bridges two B_{tet} centres, is -1.58e and this charge is similar to charges calculated for bridging O atoms in other polyborate systems. The B atoms carry positive charges of +2.25e and +2.28e (for 3- and 4-coordinate respectively) and hydroxyl O atoms on both 3- and 4-coordinate B atoms are negatively charged at -1.30e. The H atoms are positively charged at +0.52e.

The above study illustrates that it is difficult to consider computational energies of polyborate ions in isolation (gas phase), and further work is on-going in relation to computational studies involving solid-state anion-anion H-bonding interactions in extended polyborate networks.

4. Conclusions

In summary, this study has investigated the lowest energy gas phase conformations of isolated polyborate anions and all have their hydroxyl groups around trigonal B centres co-

planar with B-O bonds. In addition, the diborate (**4**) and 'O+' isomer of the heptaborate (**12**) each possess an intramolecular H-bond, with 6-membered rings. The calculated energies of the polyborate anions have been used in isodesmic calculations to determine their relative stabilities. The pentaborate(1-) anion is the most stable polyborate relative to B(OH)₃/OH⁻/H₂O building blocks, but the monoborate(1-) anion has a greater relative stability *per boron atom*. Analysis of representative solid-state crystal structures show that H-bond acceptor interactions are formed by most O atoms of these polyborate anions. These H-bond interactions are energetically significant and severely limit the use of gas phase calculations to model these isolated anions in their solid state structures.

Acknowledgment. We would like to thank a reviewer for detailed constructive comments.

References

1. C. L. Christ, J. R. Clarke, A crystal-chemical classification of borate structures with emphasis on hydrated borates, *Phys Chem. Minerals* 2 (1977) 59-87.
2. I. Tsuyumoto, T. Oshio, K. Katayama, Preparation of highly concentrated aqueous solution of sodium borate, *Inorg. Chem. Commun.* 10 (2007) 20-22.
3. G. Heller, A survey of structural types of borates and polyborates, *Top. Curr. Chem.* 131 (1986) 39-98.
4. E. L. Belokoneva, Borate crystal chemistry in terms of the extended OD theory: topology and symmetry analysis, *Crystallogr. Rev.* 11 (2005) 151-198.
5. N. P. Nies in J. W. Mellor's 'A Comprehensive Treatise on Inorganic and Theoretical Chemistry', Longmans, Green and Co., London, 5A Sup. 1 (1980) 343-501.
6. C. G. Salentine, High-field ¹¹B NMR of alkali borates. Aqueous polyborate equilibria, *Inorg. Chem.* 22 (1983) 3920-3924.

7. J. L. Anderson, E. M. Eyring, M P. Whittaker, Temperature jump rate studies of polyborate formation in aqueous boric acid, *J. Phys. Chem.* 68 (1964) 1128-1132.
8. Y. Q. Zhou, C. H. Fang, Y. Fang, Structure of supersaturated aqueous sodium pentaborate solution, *Acta Physico-Chemica Sinica* 26 (2010) 2323-2330.
9. L. Maya, Identification of polyborate and fluoropolyborate ions in solution by Raman spectroscopy, *Inorg. Chem.* 15 (1976) 2179-2184.
10. Y. Q. Zhou, C. H. Fang, Y. Fang, F. Y. Zhu, Polyborates in aqueous solution: a Raman and DFT theory investigation, *Spectrochimica Acta Part A - Molecular and Biomolecular Spectroscopy* 83 (2011) 82-87.
11. J. B. Farmer, Metal borates, *Adv. Inorg. Chem.* 25 (1982) 187-237.
12. P. T. Corbett, J. Leclaire, L. Vial, K. R. West, J.-L. Wietor, J. K. M. Sanders, S. Otto, Dynamic combinatorial chemistry, *Chem. Rev.* 106 (2006) 3652–3711.
13. M. A. Beckett, P. N. Horton, M. B. Hursthouse, D. A. Knox, J. L. Timmis, Structural (XRD) and thermal (DSC, TGA) and BET analysis of materials derived from non-metal cation pentaborate salts, *Dalton Trans.* 39 (2010) 3944-3951.
14. Gaussian 09, Revision C.01, M. J. Frisch, G. W. Trucks, H. B. Schlegel, G. E. Scuseria, M. A. Robb, J. R. Cheeseman, G. Scalmani, V. Barone, B. Mennucci, G. A. Petersson, H. Nakatsuji, M. Caricato, X. Li, H. P. Hratchian, A. F. Izmaylov, J. Bloino, G. Zheng, J. L. Sonnenberg, M. Hada, M. Ehara, K. Toyota, R. Fukuda, J. Hasegawa, M. Ishida, T. Nakajima, Y. Honda, O. Kitao, H. Nakai, T. Vreven, J. A. Montgomery, Jr., J. E. Peralta, F. Ogliaro, M. Bearpark, J. J. Heyd, E. Brothers, K. N. Kudin, V. N. Staroverov, R. Kobayashi, J. Normand, K. Raghavachari, A. Rendell, J. C. Burant, S. S. Iyengar, J. Tomasi, M. Cossi, N. Rega, J. M. Millam, M. Klene, J. E. Knox, J. B. Cross, V. Bakken, C. Adamo, J. Jaramillo, R. Gomperts, R. E. Stratmann, O. Yazyev, A. J. Austin, R. Cammi, C. Pomelli, J. W. Ochterski, R. L. Martin, K. Morokuma, V. G. Zakrzewski, G. A. Voth, P. Salvador, J. J. Dannenberg, S. Dapprich, A. D. Daniels, Ö. Farkas, J. B. Foresman, J. V. Ortiz, J. Cioslowski, D. J. Fox, Gaussian, Inc., Wallingford CT (2009).

15. D. J. Wolstenholme, C. F. Matta, T. S. Cameron, Experimental and theoretical electron density study of a highly twisted polycyclic aromatic hydrocarbon: 4-methyl-[4]helicene, *J. Phys. Chem. A* 111 (2007) 8803-8813.
16. J. Hernandez-Trujillo, C. F. Matta, Hydrogen-hydrogen bonding in biphenyl revisited, *Struct. Chem.* 18 (2007) 849-857.
17. C. F. Matta, J. Hernandez-Trujillo, T. H. Tang, R. F. W. Bader, Hydrogen-hydrogen bonding: a stabilizing interaction in molecules and crystals, *Chem. Eur. J.* 9 (2003) 1940-1951.
18. A. H. Pakiari, K. Eskandari, Closed shell oxygen-oxygen bonding interaction based on electron density analysis, *J. Mol. Struct. - THEOCHEM* 806 (2007) 1-7.
19. F. W. Biegler-Konig, J. Schonbohm, D. Bayles, AIM2000 - A program to analyze and visualize atoms in molecules, *J. Comput. Chem.* 22 (2001) 545-559.
20. F. W. Biegler-Konig, Calculation of atomic integration data, *J. Comput. Chem.* 21 (2000) 1040-1048.
21. R. F. W. Bader in *Molecules: A Quantum Theory*; Oxford University Press: Oxford, UK, (1990).
22. P. L. A. Popelier, *Atoms in Molecules: An Introduction*; Prentice Hall: London (2000).
23. C. F. Matta, R. J. Boyd (Eds); *The Quantum Theory of Atoms in Molecules: From solid State to DNA to Drug Design*; Wiley-VCH: Weinheim (2007).
24. Z.-H. Liu, L.-Q. Li, W.-J. Zhang, Two new borates containing the first examples of large isolated polyborate anions: chain $[B_7O_9(OH)_5]^{2-}$ and ring $[B_{14}O_{20}(OH)_6]^{4-}$, *Inorg. Chem.* 45 (2006) 1430-1432.
25. C.-Y. Pan, G.-M Wang, S-T. Zheng, G.-Y. Yang, Syntheses, characterizations, and crystal structures of two new organically templated borates, *Z. Anorg. Allg. Chem.* 633 (2007) 336-340.
26. M. A. Beckett, P. N. Horton, S. J. Coles, D. W. Martin, Synthesis and structural characterization of an unprecedented nonmetal cation polyborate salt containing two different "isolated" polyborate anions: $[H_2en]_2[B_4O_5(OH)_4][B_7O_9(OH)_5].3H_2O$ (en = $H_2NCH_2CH_2NH_2$), *Inorg. Chem.* 50 (2011) 12215-12218.

27. D. M. Schubert, M. Z. Visi, S. Khan, C. B. Knobler, Synthesis and structure of a new heptaborate oxoanion isomer: $B_7O_9(OH)_5^{2-}$, *Inorg. Chem.* 47 (2008) 4740-4745.
28. M. A. Beckett, P. N. Horton, M. B. Hursthouse, J. L. Timmis, K. S. Varma, Templated heptaborate and pentaborate salts of *cyclo*-alkylammonium cations: structural and thermal properties, *Dalton Trans.* 41 (2012) 4396-4403.
29. A. Becke, Density-functional thermochemistry .3. The role of exact exchange, *J. Chem. Phys.* 93 (1998) 5648-5652.
30. C. Lee, W. Yang, R. Parr, Development of the Colle-Salvetti correlation-energy formula into a functional of the electron-density, *Phys. Rev. B* 37 (1988) 785-789.
31. R. H. Hertwig, W. Koch, On the parameterization of the local correlation functional. What is Becke-3-LYP? *Chem. Phys. Lett.* 268 (1997) 345-351.
32. GaussView, Version 5, R. Dennington, T. Keith, J. Millam, Semichem Inc., Shawnee Mission KS (2009).
33. F. Biegler-König, J. Schönbohm, D. Bayles, Software news and updates - AIM2000 - a program to analyze and visualize atoms in molecules, *J. Comput. Chem.* 22 (2001) 545-559.
34. A. C. Hess, P. F. McMillan, M. O'Keeffe, Torsional barriers and force fields in H_4TO_4 molecules and molecular ions ($T = C, B, Al, Si$), *J. Phys. Chem.* 92 (1988) 1785-1791.
35. D. M. Schubert, R. A. Smith, M. Z. Visi, Studies of crystalline nonmetal borates, *Glass Technology* 44 (2003) 63-70.
36. M. Z. Visi, C. B. Knobler, J. J. Owen, M. I. Khan, D. M. Schubert, Structures of self-assembled nonmetal borates derived from α,ω -diaminoalkanes, *Cryst. Growth Des.* 6 (2006) 538-545.
37. M. A. Beckett, P. N. Horton, M. B. Hursthouse, J. L. Timmis, K. S. Varma, Synthesis, characterization, and thermal properties of benzylammonium pentaborate $[C_6H_5CH_2NH_3][B_5O_6(OH)_4]$, *Collect. Czech. Chem. C.* 75 (2010) 2832-2838.
38. M. A. Beckett, C. C. Bland, P. N. Horton, M. B. Hursthouse, K. S. Varma, Supramolecular structures containing 'isolated' pentaborate anions and non-metal

cations: crystal structures of $[\text{Me}_3\text{NCH}_2\text{CH}_2\text{OH}][\text{B}_5\text{O}_6(\text{OH})_4]$ and $[\text{4-MepyH}, \text{4-Mepy}][\text{B}_5\text{O}_6(\text{OH})_4]$, *J. Organomet. Chem.* 692 (2007) 2832-2838.

39. M. C. Etter, Encoding and Decoding hydrogen-bond patterns of organic compounds, *Accounts Chem. Res.* 23 (1990) 120-126.

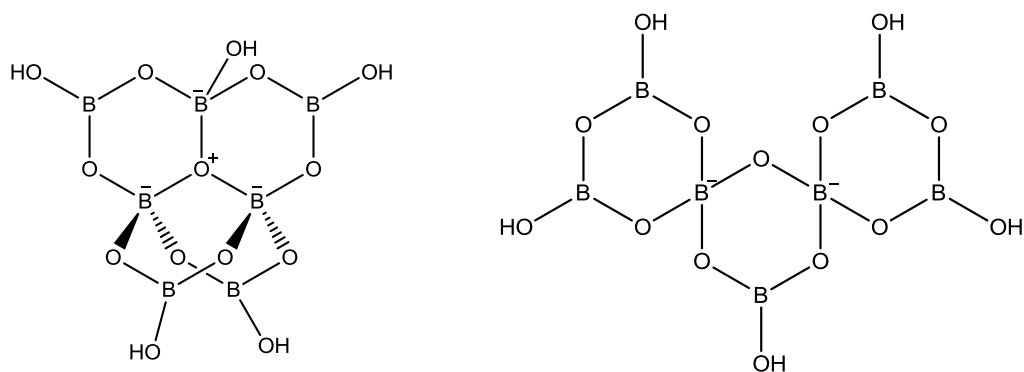


Figure 1. The two isomeric forms of the $[\text{B}_7\text{O}_9(\text{OH})_4]^{2-}$ anion. The structure on the left is referred to in this article as the ‘O⁺’ isomer and the one on the right as the ‘ribbon’ isomer.

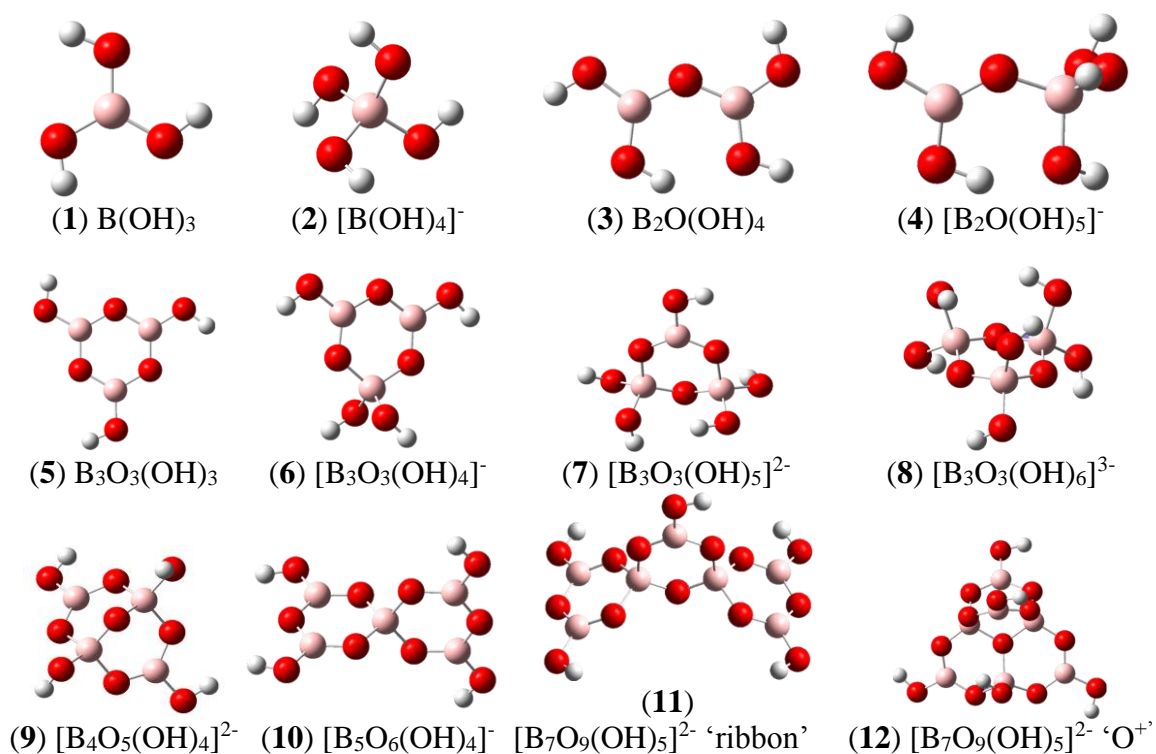
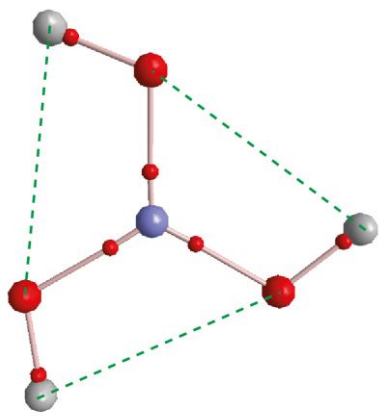
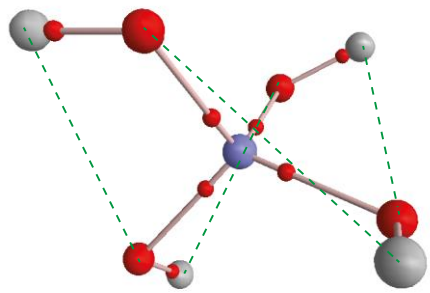


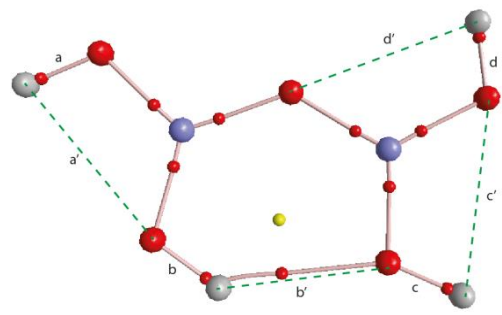
Figure 2. Optimised structures of the polyborates at B3LYP/6-311++G(*d,p*). Energies (au) are as follows: **1** (-252.588496), **2** (-328.492215), **3** (-428.713412), **4** (-504.642425), **5** (-528.362535), **6** (-604.300174), **7** (-680.069710), **8** (-755.695015), **9** (-779.742810), **10** (-880.106381), **11** (-1231.715105), **12** (-1231.711950).



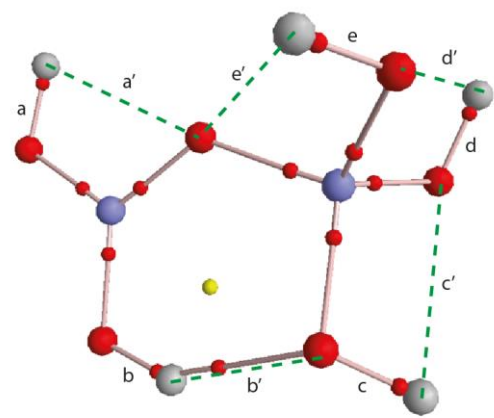
(1)



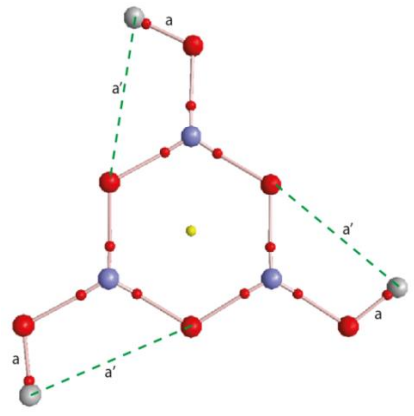
(2)



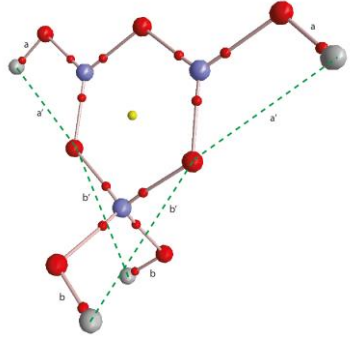
(3)



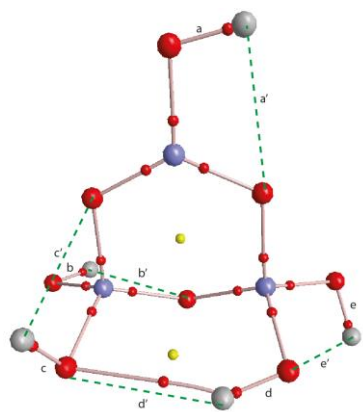
(4)



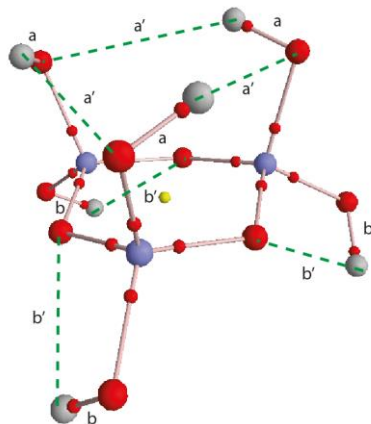
(5)



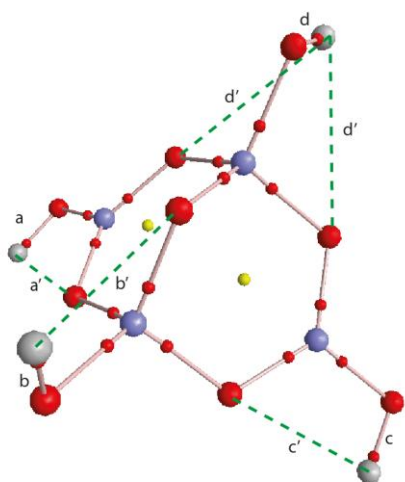
(6)



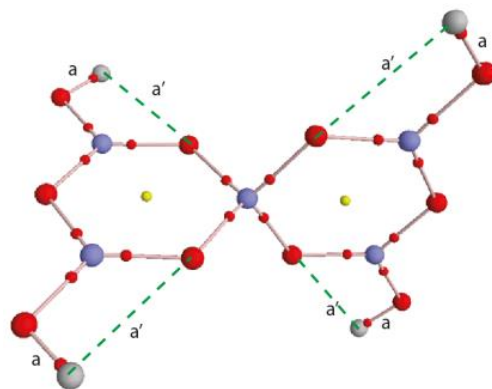
(7)



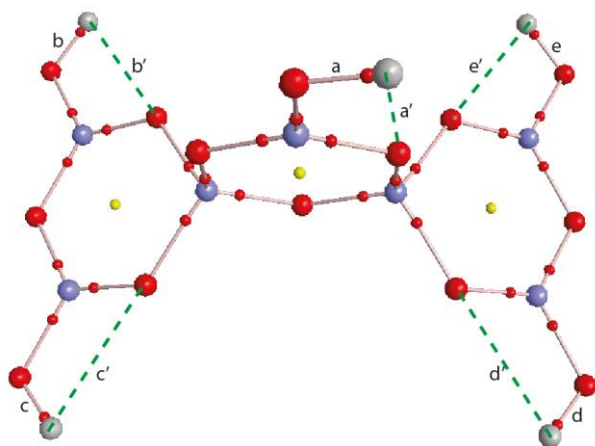
(8)



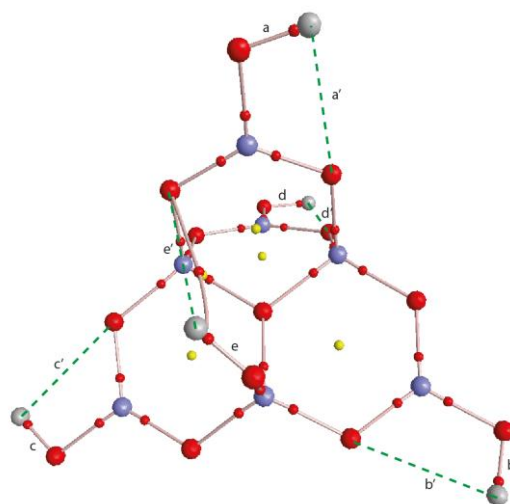
(9)



(10)



(11)



(12)

Figure 3. QTAIM molecular graphs for selected polyborate minima depicting bond paths (red lines), bond (red dots) and ring (yellow dots) critical points.